Improvement of a dynamic scanning force microscope for highest resolution imaging in ultrahigh vacuum

S. Torbrügge,[1] J. Lübbe,[1] L. Tröger,[1] M. Cranney,[1] T. Eguchi,[2] Y. Hasegawa,[2,3] and M. Reichling[1,a)]

[1]*Fachbereich Physik, Universität Osnabrück, Barbarastraße 7, 49076 Osnabrück, Germany*
[2]*The Institute for Solid State Physics, The University of Tokyo, 5-1-5 Kashiwa-no-ha, Kashiwa 277-8581, Japan*
[3]*PRESTO, Japan Science and Technology Agency, Chiyoda-ku, Tokyo 102–0075, Japan*

(Received 2 April 2008; accepted 2 July 2008; published online 4 August 2008)

We report on a modification of a commercial scanning force microscope (Omicron UHV AFM/STM) operated in noncontact mode (NC-AFM) at room temperature in ultrahigh vacuum yielding a decrease in the spectral noise density from 2757 to 272 fm/$\sqrt{\text{Hz}}$. The major part of the noise reduction is achieved by an exchange of the originally installed light emitting diode by a laser diode placed outside the vacuum, where the light is coupled into the ultrahigh vacuum chamber via an optical fiber. The setup is further improved by the use of preamplifiers having a bandpass characteristics tailored to the cantilever resonance frequency. The enhanced signal to noise ratio is demonstrated by a comparison of atomic resolution images on $CeO_2(111)$ obtained before and after the modification. © *2008 American Institute of Physics.* [DOI: 10.1063/1.2964119]

I. INTRODUCTION

The dynamic scanning force microscope (SFM) operated in the noncontact atomic force microscopy (NC-AFM) mode in an ultrahigh vacuum (UHV) environment has become a standard tool in surface science for the characterization of insulating materials at the atomic scale.[1–4] Continuous improvement of the instrumentation in the rapidly developing field of SFM have been achieved, enabling not only the studies of surfaces at the atomic scale but also the chemical identification[5] and manipulation of single atoms[6] and molecules.[7]

In this contribution we demonstrate how the spectral noise density of a commercial scanning force microscope [UHV AFM/STM, Omicron, Taunusstein, Germany; based on a design of Howald *et al.*[8]] operated in ultrahigh vacuum can be decreased from 2757 fm/$\sqrt{\text{Hz}}$ measured for the original setup to 272 fm/$\sqrt{\text{Hz}}$ for the modified setup. The setup is based on detecting the cantilever oscillation by the optical beam deflection (OBD) method, which is predominantly used in SFM.[3] The reduced noise density is achieved by an exchange of the originally installed light emitting diode (LED) by a fiber-coupled laser diode (LD). Furthermore, an *ex situ* preamplifier with an optimized bandpass characteristics is installed. The enhanced atomic resolution imaging capabilities of the modified setup are demonstrated by atomic resolution SFM measurements on $CeO_2(111)$.

II. MODIFICATION OF THE OBD SETUP

In this section we describe the modification of the OBD setup in detail. Two photographs of the microscope stage before (A) and after (B) the exchange of the LED by a LD are shown in Fig. 1. In the original setup the LED is installed on top of the housing (1) containing two adjustable mirrors to guide the light beam onto the cantilever and the position sensitive detector (PSD). The PSD is a quadrant photodetector [Fig. 1(c)]. For this microscope design, the cantilever is fixed in its position and the sample is scanned in front of the tip by the sample scanner (2) opposite to the housing of the PSD.[8] The originally installed LED is replaced by a metal cylinder of the same dimensions [Fig. 1(b)] which locks an optical fiber via a piece of slashed Viton cut from an O-ring [Fig. 1(c)]. The light is introduced into the SFM optical system via a single mode optical fiber (SMC, Schäfter und Kirchhoff, Hamburg, Germany) that is protected against mechanical damage by a U-shaped stainless steel tube with an inner diameter of 1 mm [Fig. 1(b)].

The alignment of the laser beam onto the cantilever and the PSD is achieved by two motorized mirrors[9] A schematic picture of the optical path is shown in Fig. 1(c). The beam divergence at the fiber end is reduced by a lens system (we use the originally installed lens system) focusing the light beam onto the cantilever. The first mirror guides the light beam from the optical fiber onto the cantilever back side. The light is reflected from the cantilever toward a second motorized mirror that guides the beam to the center of the PSD.[8]

A. The light source

The original light source is a LED placed inside the UHV (Ref. 8) [Fig. 1(a)]. The LED can withstand bakeout temperatures up to 125 °C, which is essential for the bakeout of the system to achieve UHV conditions. The drawback of a LED is, however, the low light power and the strongly divergent beam. The LED provides a maximum light power

a)Electronic mail: reichling@uos.de.

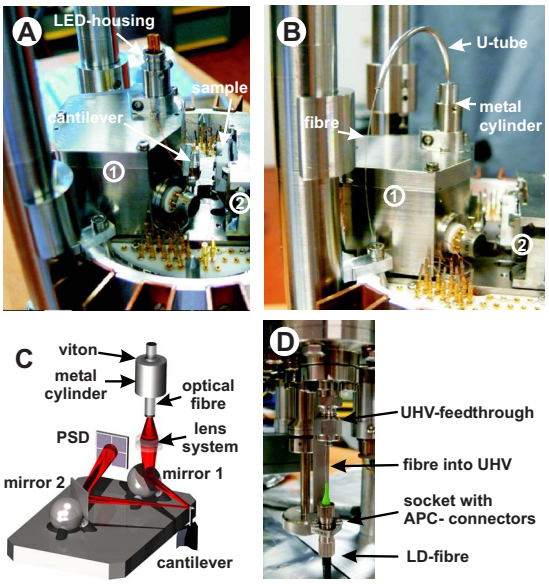

FIG. 1. (Color online) (a) Photograph of the AFM scan head with the originally installed LED. (b) Scan head after exchanging the LED by a metal cylinder of same dimensions used to attach an optical fiber to the former LED housing. A U-shaped stainless steel tube protects the fiber from mechanical damage. (1) Housing for the mirrors and the PSD. (2) Sample scanner. (c) Schematic drawing of the modified optical beam deflection setup. The originally installed LED is replaced by a fiber-coupled LD. The light from the fiber is focused by a set of lenses (same as for the LED) and directed onto the cantilever back side by mirror 1. The reflected beam is centered onto the PSD by mirror 2. The optical fiber is fixed by a piece of slashed Viton cut from an O-ring to the metal cylinder replacing the originally installed LED. (d) Photograph of the homebuilt UHV feedthrough for the optical fiber. The fiber-coupled LD can be connected to the UHV feedthrough by the APC connector.

of 1.15 mW and the beam divergence is so high that the focus of the beam is much larger than the cantilever width.

As the new light source we use a fiber-coupled intensity and temperature controlled LD operating at $\lambda=685$ nm (48TE-SOT, Schäfter und Kirchhoff), placed outside the vacuum chamber. This is because LDs do not withstand temperatures above 100 °C. The laser light is guided into the UHV chamber via an optical fiber.

Back reflections of the laser light into the laser cavity may result in unstable operation conditions, leading to additional noise and possibly a destruction of the LD. This so-called optical feedback noise is minimized in our case by the use of a Faraday isolator (48FI-5–670, Schäfter und Kirchhoff), an optical component which allows the transmission of polarized light in only one direction. In addition we use fiber connectors with an angled physical contact (APC) connector type having an 8° angled polish at the fiber end (equals fiber ferrule) (Schäfter und Kirchhoff) to further reduce back reflections into the LD.

The LD working point is optimized for low noise operation at a relatively large intensity. Instead of reducing the laser power by adjusting the operation current, the beam intensity is adjusted by a mechanical attenuator reducing the beam cross section (48AT, Schäfter und Kirchhoff). Thus low noise operation of the LD at any desired intensity is guaranteed. The measured light power fluctuations at the end of the FC/APC connector of the optical fiber are below 1%/h.

The increased laser power up to 10 mW of the LD enables us to use cantilevers without reflex coating. Reflex coatings result in decreased quality factors Q in comparison to the same cantilever type without any coating. Previously, we used reflex coated cantilevers (PPP-QFMR, Nanosensors, Neuchatel, Switzerland) having typical quality factors ranging from 30 000 to 100 000 when the LED was applied as the light source. After installation of the LD, we can use the same cantilever type without reflex coating (PPP-FM, Nanosensors) with measured Q values in the range of 50 000–200 000. The use of such high Q probes results in an enhanced force sensitivity in NC-AFM imaging.[10]

B. Optical fiber

The use of an optical fiber with a FC/APC connector at the end outside the vacuum chamber facilitates the disconnection to the LD from the vacuum system during bakeout [Fig. 1(d)]. The other end attached to the microscope head in the UHV [Figs. 1(b) and 1(c)] is cut perpendicular. The optical core of the fiber is protected by an acrylic buffer. The acrylic buffer is withstanding the necessary bakeout temperatures of about 120 °C and has been found not to outgas. To ensure a very small laser spot size on the cantilever we chose a fiber with 4.7 μm mode field diameter (beam diameter at the fiber exit) and a numerical aperture of NA=0.10 corresponding to an opening angle of the light beam at the end of the perpendicular cut fiber of 11.5°.

Special care has been taken to produce a highest quality cleaved surface at the end of the fiber. We used a fiber cutter with an electronically tuned ultrasonic blade FK11 (Photon Kinetics, Beaverton, USA). Thus, we yield a nearly Gaussian spot profile at the end of the fiber with a few speckles due to light scattering at the cleaved surface. The measured loss of light power at the fiber end compared to the laser power measured directly at the fiber connector of the LD is below 10%.

The laser beam is focused on the back side of the cantilever by a set of lenses (we use the originally installed lens system [Fig. 1(c)]). The position of the metal cylinder holding the fiber can be varied to adjust for the smallest spot size. The cylinder is fixed by a screw.

A smaller spot size allows to collect much more light reflected from the cantilever for detection by the PSD for the setup with the LD than for the setup with the LED. The small laser spot can be well positioned on the front end of the cantilever resulting in an increased signal to noise ratio.

C. UHV feedthrough

The laser light from the LD is guided into the UHV chamber by an optical fiber via the APC fiber connector (60C-FC/FC, Schäfter und Kirchhoff). This connector is plugged into a socket mounted on an UHV feedthrough [Fig. 1(d)]. Another piece of fiber guides the light from the socket to the scan head. We use a homebuilt feedthrough based on a design avoiding the necessity to glue the optical fiber.[11] The feedthrough consists of a fitting (Swagelok, Solon Ohio, USA) welded onto a 16 CF flange and a conically shaped Teflon ferrule. The fiber is passed through a center-drilled

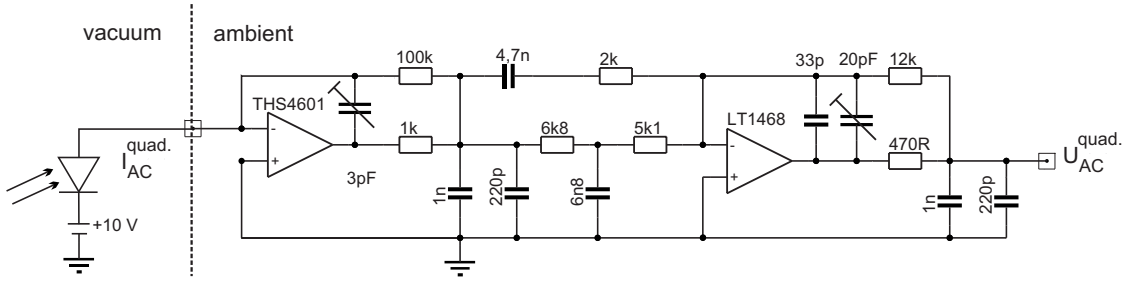

FIG. 2. Circuit diagram of the current-to-voltage converter and first amplification stage used for each of the four PSD quadrants. A voltage converter with low-pass filter characteristics reducing high frequency noise is followed by an amplification stage having bandpass characteristics.

hole in the Teflon ferrule. The drilling of 0.30 mm in diameter is slightly larger than the fiber diameter of 0.25 mm. The Teflon cone acts as a gasket as it is pressed to the Swagelok fitting by means of a nut reducing the diameter of its drilling. This feedthrough allows operation of the system at a pressure below 10^{-10} mbar and withstands frequent bakeout at 120 °C. Since also mounting of the fiber to the scan head does not require gluing, it is straightforward to exchange the fiber in case of damage. In this case solely the Teflon cone has to be exchanged.

D. Preamplifier

The photocurrent from the PSD that is alternating due to the cantilever oscillation is converted to an ac voltage with a preamplifier directly attached to the base flange of the microscope head outside the UHV chamber. We designed preamplifiers suited for the needs of high resolution SFM measurements replacing the originally installed preamplifier.

Besides using lowest noise components for the new preamplifiers, the main improvement is to adapt the frequency response of the transimpedance to the resonance frequencies of the cantilevers used. A circuit diagram of the current-to-voltage converter with subsequent bandpass amplification used for each PSD quadrant [Fig. 1(c)] is presented in Fig. 2. First the PSD current I_{ac}^{quad} is converted with low-pass characteristics to an ac voltage suppressing high frequency noise. In a second step the voltage signal is amplified with a frequency dependent gain having bandpass characteristics tailored to the resonance frequency of the used cantilever to yield the output voltage U_{ac}^{quad}. Thus low frequency noise ($1/f$ noise[2] and noise from mechanical vibrations) is significantly reduced.

Figure 3 shows the transimpedance $Z^{quad}=U_{ac}^{quad.}/I_{ac}^{quad.}$ of the preamplifiers where the frequency response of the originally installed preamplifier is shown in Fig. 3(a). As can be seen the original preamplifier exhibits a low-pass characteristics. This design has the major disadvantage that low frequency noise is more amplified than the oscillation signal of the cantilever having a resonance frequency typically between 50 and 500 kHz. The resonance frequencies of cantilevers used in our experiments are indicated by dashed lines. The low-pass characteristics hampers the use of stiff cantilevers having a resonance frequency of typically 270 kHz. This is the reason why in our earlier work exclusively cantilevers with resonance frequencies of about 75 kHz were used.[12–14]

The new preamplifiers with bandpass characteristics have been optimized for operation at cantilevers having eigenfrequencies of about 90 and about 270 kHz. The corresponding frequency response curves of the transimpedance are shown in Fig. 3(b). The bandpass characteristics enable a selective amplification of the cantilever oscillation signal while lower and higher frequency noise is attenuated. This design is very suitable for high resolution imaging at the first cantilever resonance frequency. However, it is not suitable for parallel measurements at the first resonance frequency and higher harmonics, since the amplification at high frequencies is too low to pick up the higher harmonics signals. For such applications, a high bandwidth preamplifier is needed.

III. PERFORMANCE TEST

A. Sensitivity and noise figures

First, we relate the light power at the end of the fiber connector measured with an optical power meter (TQ8210 equipped with a fiber adapter, Advantest, Tokyo, Japan) as a function of the signal U_Σ defined as the sum of the signals of all four quadrants of the PSD. The respective dependency is depicted in Fig. 4(a), whereby a cantilever without reflex coating (PPP-FM, Nanosensors) was used for this and all further measurements in Sec. III A, if not stated otherwise. From Fig. 4(a) it is evident that U_Σ increases linearly with light power indicating that even for a light power of 1 mW, the PSD is not in saturation. For comparison, also the sum signal for the originally installed LED operated at maximum current, a set point which has normally been used in experiments, is indicated. In the LED configuration, for a light

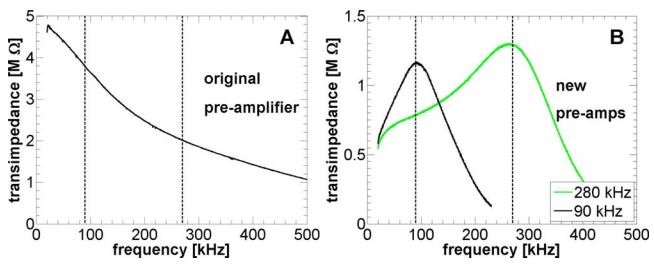

FIG. 3. (Color online) Frequency dependence of the transimpedance (current-to-voltage conversion) (a) of the originally installed preamplifier and (b) the two new preamplifiers optimized for resonance frequencies of about 90 kHz and about 270 kHz [marked by dotted vertical lines in (a) and (b), respectively].

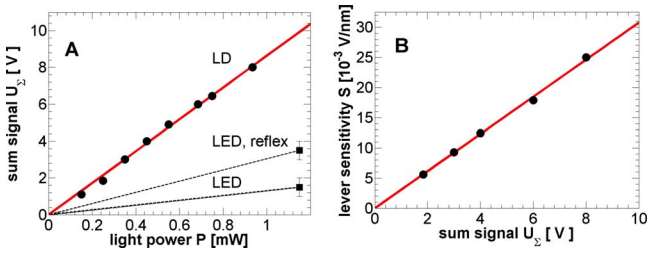

FIG. 4. (Color online) (a) Measured PSD sum signal U_Σ as a function of laser light power coupled into the FC/APC connector. (b) Optical lever sensitivity S as a function of U_Σ. Solid lines represent linear least-squares fits to the data. Dashed lines in (a) are a guide to the eye. LD: when the laser diode and uncoated cantilevers are used; LED: using LED with uncoated cantilevers; LED reflex: using LED and reflex coated cantilevers.

power of 1.15 mW a sum voltage of only about 1.5 V has been measured if cantilevers without any reflex coating were used. High-Q cantilevers with reflex coatings (PPP-QFMR, Nanosensors) were used in our earlier work[12,13] to increase the signal to 3.5 V. As a major improvement we note that at the same applied light power of about 1 mW the sum signal is by a factor of 6 larger for the LD ($\simeq$9 V) compared to the LED ($\simeq$1.5 V) without the use of reflex coated cantilevers. We ascribe this increase in light power on the PSD to the smaller divergence of the laser beam compared to the LED.

To estimate the oscillation amplitude of an either thermally or mechanically excited cantilever, it is necessary to calibrate the sensitivity of the setup. The optical lever sensitivity S is defined as $S=\Delta V/\Delta A$, with the detector voltage changes ΔV and the change in cantilever oscillation amplitude ΔA. The lever sensitivity is obtained by plotting the voltage for driving the oscillation as a function of the variation of the vertical displacement for keeping constant a given value of the normalized frequency shift.[15,16] The slope of such an amplitude versus displacement plot corresponds to the sensitivity S. The optical lever sensitivity has to be determined every time the light intensity or the spot position on the cantilever is changed. Figure 4(b) shows S for the same cantilever and fixed light spot position as a function of U_Σ, whereas U_Σ is proportional to the applied light power. Hence, we find that the optical lever sensitivity S is directly proportional to the applied laser power P.

To quantify the noise, we measure the thermally excited cantilever motion, determine the optical lever sensitivity S, and calculate the deflection noise density D_{ND} as described below. In Sec. III A all experiments characterizing the original LED setup were done using the originally installed preamplifier. Measurements for the LD setup have been done using the new preamplifier optimized for 90 kHz cantilevers. The voltage spectral density $U_{SD}(f)$ of the thermally excited cantilever oscillation is measured with a spectrum analyzer (SR 770, Stanford Research Systems, Sunnyvale, USA). Typical spectra of the thermally excited cantilever vibrations are shown in Figs. 5(a) and 5(b) using the original setup and the new setup (LD and new preamplifier) as the light source, respectively. The resonance peak can clearly be identified in both spectra. It is evident by a direct comparison of both spectra that the resonance peak measured when the new setup is used [Fig. 5(b)] is much more pronounced than the

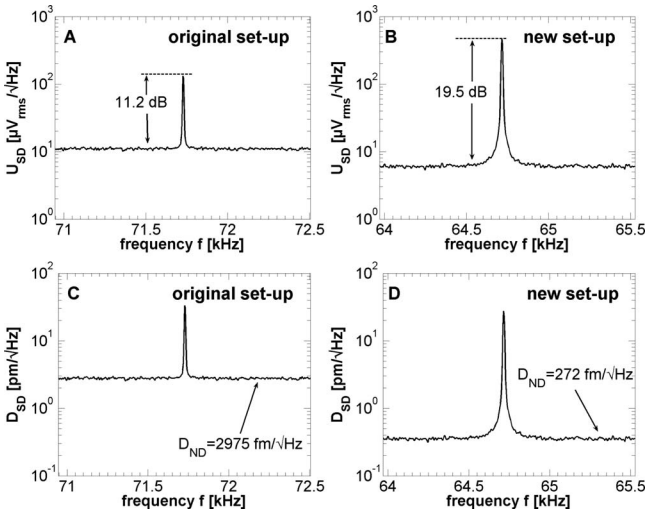

FIG. 5. Voltage spectral densities U_{SD} of the thermally excited cantilever oscillation measured with the LED (a) and the LD (b) as the light source together with the respective deflection spectral densities D_{SD} shown in (c) and (d). The optical lever sensitivity was measured to be S_{LED} =0.0041 V/nm at U_Σ^{LED}=3.2 V and S_{LD}=0.0170 V/nm at U_Σ^{LD}=6.0 V. For LED measurements, silicon cantilevers from Nanosensors, PPP-QFMR with reflex coating, and for the LD measurements, uncoated PPP-FM were used. Both cantilever types had the same nominal force constant of k=2.8 N/m, resonance frequencies of f_0^{LED}=71 738 Hz and f_0^{LD} =64 710 Hz and the quality factors were measured to be Q_{LED}=72 325 and Q_{LD}=69 300.

peak using the original setup [Fig. 5(a)]. The signal to noise ratio calculated from the ratio of peak height to the noise floor for the original setup amounts 11.2 dB, while it is 19.5 dB for the new setup.

To characterize the quality of the OBD oscillation detection setup, we determine the deflection noise density D_{ND} which corresponds to the noise floor of the deflection spectral density D_{SD} in the oscillation spectrum of a thermally excited cantilever.[15,17] The noise floor is a measure for the smallest detectable oscillation signal of the setup. To accomplish this, we calibrate the optical lever sensitivity S for a measured voltage spectral density U_{SD} and extract the deflection spectral density D_{SD} in the units [fm/$\sqrt{\text{Hz}}$] from the voltage spectral density U_{SD} measured in the units [V/$\sqrt{\text{Hz}}$] by the relation

$$D_{SD} = U_{SD}/S. \tag{1}$$

This was done for both spectra shown in Figs. 5(a) and 5(b) and the corresponding deflection spectral densities are plotted in Figs. 5(c) and 5(d). The optical lever sensitivity for the measurement using the LED was S=0.0041 V/nm yielding a deflection noise density of D_{ND}=2975 fm/$\sqrt{\text{Hz}}$ calculated from the voltage noise floor of 12.2 μV/$\sqrt{\text{Hz}}$ in Fig. 5(a). The spectrum was recorded at a light intensity of 1.15 mW corresponding to U_Σ=3.2 V. The optical lever sensitivity for the measurement using the LD was S=0.017 V/nm yielding D_{ND}=272 fm/$\sqrt{\text{Hz}}$ calculated from the voltage noise floor of 4.7 μV/$\sqrt{\text{Hz}}$ in Fig. 5(d). The spectrum was recorded at a light intensity of 0.7 mW corresponding to U_Σ=6 V.

To explore the feasible range of laser intensities, we determined the deflection noise density D_{ND} from the noise floor in D_{SD} at various laser power levels, where the corre-

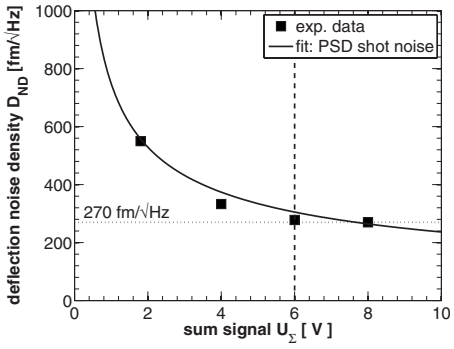

FIG. 6. Deflection noise density as a function of U_Σ. The solid line represents a least-squares fit to the experimental data according to Eq. (2). The dashed line corresponds to the sum signal typically used for NC-AFM experiments. A silicon cantilever (PPP-FM, Nanosensors) $f_0=74\,720$ Hz, $Q=69\,930$, and $k=2.8$ N/m was used.

sponding plot for one cantilever is shown in Fig. 6. With increasing light power, the noise floor monotonously decreases and attains a level below 270 fm/$\sqrt{\text{Hz}}$ for $U_\Sigma > 6$ V. The optical lever sensitivity S increases linearly with the applied light power P and, therefore, according to Eq. (1) the deflection spectral density is proportional to $1/P$. However, the major noise in an OBD setup is the photodetector shot noise which is proportional to $\sqrt{P}$.[18] An in-depth treatment of the problem shows that the overall deflection noise density D_{ND} caused by shot noise is given by

$$D_{\text{ND}} = \frac{la}{3s}\sqrt{\frac{2e}{\eta}}\sqrt{\frac{1}{P}} = m\sqrt{\frac{1}{P}}, \tag{2}$$

where l is the cantilever length, a is the laser spot diameter on the PSD, s is the cantilever to PSD distance, e is the elementary charge, and η is the efficiency of the light-to-current conversion of the PSD.[17] For a given cantilever, all parameters in Eq. (2) except P are constants that can be combined into one constant of proportionality m. A corresponding least-squares fit of Eq. (2) with the fit parameter m to the experimental data is drawn as a solid line in Fig. 6. The good agreement of the experimental data to the fit suggests that our OBD setup has shot noise limited performance. We conclude from Fig. 6 that for our modified OBD setup the noise level cannot be reduced strongly by operating the system at a voltage close to the upper limit of $U_\Sigma=10$ V. As unwanted heating of the cantilever increases with laser power, we use a value of $U_\Sigma=6$ V as a good trade-off between increased sensitivity and cantilever heating.

We quantified D_{ND} of our system before we exchanged the LED in the same way for several cantilevers, yielding as the best value 2757 fm/$\sqrt{\text{Hz}}$. Finally we also compared the performance of the new preamplifier to the originally installed preamplifier when the LD was used as the light source. The best achieved values for all tested configurations are shown in Table I. The deflection noise density is decreased from 545 to 272 fm/$\sqrt{\text{Hz}}$, for a change from the original preamplifier to the homebuilt preamplifier. Altogether the noise level is decreased by one order of magnitude for our new setup in comparison to the original configuration.

TABLE I. Deflection noise densities D_{ND} obtained for the different tested setups before and after the modification.

Light source	Preamplifier	Cantilever	D_{ND} (fm/$\sqrt{\text{Hz}}$)
LED	Original	75 kHz, coated	2757
LD	Original	75 kHz, uncoated	545
LD	New 90 kHz	75 kHz, uncoated	272

The achieved deflection noise density of 270 fm/$\sqrt{\text{Hz}}$ is comparable to the noise levels of the best interferometric cantilever oscillation detection systems[2] and optimized quartz tuning fork systems having a spectral noise density of typically 170 fm/$\sqrt{\text{Hz}}$ (Ref. 15) when operated in UHV.

We also compare the noise in the detection of the detuning signal Δf at the output channel of the phase locked loop demodulator.[19] The decreased noise level is expressed in the detuning noise detected for the cantilever free oscillation, when the cantilever is excited at a constant oscillation amplitude of $A=15$ nm far away from the surface. Under typical experimental conditions, a fluctuation of 1 to 2 Hz was registered before the modification of the setup compared to a value of about 0.2 Hz for the modified setup.

B. Improvement in atomic resolution imaging

We demonstrate the enhanced capabilities of our new setup by imaging the $CeO_2(111)$ surface with atomic resolution similar to our previous studies.[12,13,20] The *ex situ* polished surface is prepared by repeating cycles of *in situ* Ar^+ ion sputtering (1.5 keV, 5×10^{-5} mbar, 5 min) at room temperature and successive annealing for 1 min at 1175 K.[12]

We conducted atomic resolution measurements before and after the modification with cantilevers having the same mechanical properties under similar experimental conditions. We use *p*-doped silicon cantilevers with reflex coating (PPP-QFMR, Nanosensors) and uncoated (PPP-FM) with a nominal force constant of $k\approx2.8$ N/m and a resonance frequency of about 75 kHz and uncoated high frequency cantilievers (PPP-NCH) having a resonance frequency of about 270 kHz and $k\approx42$ N/m. Tips were prepared *in situ* by Ar^+ ion sputtering (0.5 kV, 5×10^{-5} mbar, 3 min) prior to the experiments to remove the native oxide layer. However, a clean tip is most reactive and we anticipate that the imaging cluster at the tip end is a hydroxyl cluster formed from constituents of the residual gas or adsorbates on the surface.[21] The microscope is operated[19,22] in the frequency modulation detection mode (FM-AFM),[10] keeping the cantilever oscillation amplitude constant and the overall tip-surface electrostatic interaction minimized.

When comparing NC-AFM images taken under different experimental conditions, it has to be emphasized that the atomic tip termination has a strong influence on imaging quality and results may strongly differ from one measurement to the next even on the same day using the same tip. This is because contrast formation is dependent on the tip cluster structure[21] and subtle changes in the tip termination may result in a dramatically enhanced resolution compared to measurements performed under nominally identical

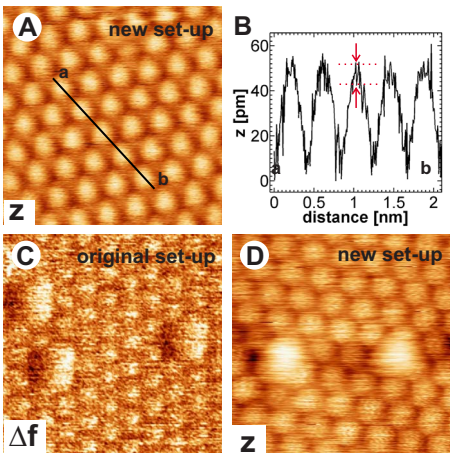

FIG. 7. (Color online) SFM images (raw data) of the $CeO_2(111)$ surface. (a) Topographic image obtained with the new setup. (b) Height profile along the solid line in (a). The noise in the topographic signal is below 8 pm as indicated by arrows. (c) and (d) show adsorbed water molecules imaged with the old and new setups, in the constant height and topographic mode, respectively. Image sizes (a), (c), and (d) 3.0×3.0 nm^2. Imaging parameters: image (a) f_0=263 855 Hz (PPP-NCH, Nanosensors), k=42.0 N/m, Q=31 251, A=16.3 nm, image set point $\Delta f_{(A)}$=−36.8 Hz, normalized frequency shift (Ref. 2) $\gamma_{(A)}$=−12.2 fN$\sqrt{\text{m}}$, fast direction scanning speed v=12 nm/s. Image (c) f_0=79 988 Hz (PPP-QFMR, Nanosensors), k=2.8 N/m, Q=63 245, A=32.5 nm, $\Delta f_{(C)}$=−14.4 Hz, $\gamma_{(C)}$=−3.0 fN$\sqrt{\text{m}}$, and v=24 nm/s. Image(d) f_0=83 898 Hz (PPP-FM, Nanosensors), k=2.8 N/m, A=36.4 nm, Q=86 259, $\Delta f_{(D)}$=−19.4 Hz, $\gamma_{(D)}$=−4.5 fN$\sqrt{\text{m}}$, and v=22.2 nm/s.

conditions.[23] Hence, one has to be careful to compare the quality of atomic resolution images obtained before and after the modification. Therefore, to evaluate improvement in atomic resolution capability we select the best images obtained before and after the modification.

For the original setup, best image quality was obtained in the constant height mode, where the distance between tip and sample is kept constant by reducing the response time of the distance feedback loop such that only the inclination between tip and sample is compensated but the feedback is not fast enough to yield atomic contrast in the topography signal.[12] In this imaging mode the detuning signal (Δf) reveals the atomic information.[12] Imaging the surface in the topographic mode (z) using the detuning signal as the feedback signal often resulted in instable imaging conditions due to the high noise level in the detuning signal. After the modification, the best results are obtained with the topography mode, using the detuning signal as the feedback signal for the topography feedback. Thus, the detuning value is kept constant and the topography (z) reflects the atomic information.

Figure 7(a) shows the stoichiometric $CeO_2(111)$ surface imaged with an uncoated silicon tip (PPP-NCH, Nanosensors) having a resonance frequency of f_0=263 855 Hz and a nominal force constant of k=42.0 N/m. It was obtained at a fast scanning speed of 12 nm/s using the new preamplifier optimized for frequencies around 270 kHz. This image represents the best contrast and signal to noise ratio we have ever obtained on this surface at room temperature. The noise in the topographic channel estimated from the line profile shown in Fig. 7(b) is below 8 pm as indicated by arrows for a corrugation of about 55 pm. This results in a relative error below 15%. The best atomic resolution images obtained on this surface in the constant height mode with the original setup showed a relative error in the detuning signal of about 30%.[21] According to the formulae describing noise figures in NC-AFM (Ref. 2) the use of stiff cantilevers having resonance frequencies of about 270 kHz and spring constants larger than 40 N/m facilitates imaging the surface with small oscillation amplitudes ($\leq$15 nm) and results in enhanced imaging quality in agreement with our experimental observation.

With the new setup we can scan in the topographic mode with atomic resolution in the z-channel with the same scanning speed in fast scan direction of about 24 nm/s as in the constant height mode what has not been possible before the modification. The advantage of the topographic mode becomes evident when protruding adsorbates are imaged on the surface. In Figs. 7(c) and 7(d) we present images of individual water molecules adsorbed on the surface.[13] Image (C) is measured with the old setup and allows the identification of three individual molecules. The image quality is the same as the best of our published data.[13] However, scanning protruding adsorbates in the constant height mode results in a strong contrast on top of the water molecules [Fig. 7(c)] but the ionic lattice appears rather faint and noisy. Also the actual shape of the water molecules is not clearly recognized. This is because the tip is in close approach to the protruding adsorbate but at a larger separation to the substrate. Scanning at closer tip-surface distance in order to image also the ionic lattice with enhanced resolution often results in instabilities due to disturbance of the tip by the adsorbates.

Image (D) is recorded with the new setup and enables us to precisely determine the shape and adsorption geometry of individual molecules since also the surface ions of the substrate appear with strong contrast. From this image we can clearly deduce that water molecules adsorb at threefold bridge positions occupying three ionic lattice sites and exhibit a symmetric triangular shape. The slightly granular structure decorating the ionic sites [Fig. 7(d)] is due to a slightly too fast topography feedback. To avoid any contact or disturbance of the tip with the adsorbed molecules, a fast feedback proved advantageous when imaging the protruding molecules. For an adsorbate-substrate system, imaging of protruding defects in the topographic mode clearly leads to an enhanced resolution in comparison to imaging in the constant height mode. The reason why the ions of the substrate and the water molecules can be nicely identified in Fig. 7(d) is that the tip followed the topography so that the tip-surface distance was sufficiently small above the molecule and the atoms of the clean surface to yield a strong contrast.

Similarly, excellent results showing enhanced resolution have been obtained in a likewise modified Omicron UHV AFM/STM microscope when imaging semiconducting surfaces.[24,25] Other groups succeeded to improve the image quality obtained with this instrument by exchanging the LED by a fiber-coupled superluminescent laser diode;[26,27] however, noise figures before and after the modification have not been reported.

IV. CONCLUSION

In this work we present modifications of a commercial AFM (Omicron UHV AFM/STM) operated in UHV leading to significantly enhanced resolution in NC-AFM experiments. We demonstrate that the exchange of the LED by a fiber-coupled LD in conjunction with an exchange of the preamplifier results in a decrease in the deflection noise density by one order of magnitude. The achieved noise level of 270 $\mathrm{fm}/\sqrt{\mathrm{Hz}}$ under UHV conditions for our modified setup is comparable to the noise levels of interferometric cantilever oscillation detection and that of a quartz tuning fork. Nevertheless, for applications of SFM in liquids, noise levels of the optical beam deflection setup below 20 $\mathrm{fm}/\sqrt{\mathrm{Hz}}$ have been reported.[17,18] This is another order of magnitude smaller than the noise level reported in this work. To further improve the OBD setup one could design an UHV suited preamplifier directly attached to the photodetector, use a radio frequency modulated laser source, and further optimize the optical path, e.g., by using an aspheric lens resulting in an elliptically shaped light spot on the PSD.[17]

ACKNOWLEDGMENTS

The authors would like to thank T. Kunstmann, M. Fendrich, Th. Glatzel, and O. Custance for most valuable discussions. Financial support from the Deutsche Forschungsgemeinschaft is gratefully acknowledged.

[1] C. Barth and M. Reichling, Nature (London) **414**, 54 (2001).
[2] F. J. Giessibl, Rev. Mod. Phys. **75**, 949 (2003).
[3] S. Morita, R. Wiesendanger, and E. Meyer, *Noncontact Atomic Force Microscopy, NanoScience and Technology* (Springer, Berlin, 2002).
[4] R. García and R. Pérez, Surf. Sci. Rep. **47**, 197 (2002).
[5] Y. Sugimoto, P. Pou, M. Abe, P. Jelinek, R. Perez, S. Morita, and O. Custance, Nature (London) **446**, 64 (2007).
[6] Y. Sugimoto, M. Abe, S. Hirayama, N. Oyabu, O. Custance, and S. Morita, Nat. Mater. **4**, 156 (2005).
[7] S. Hirth, F. Ostendorf, and M. Reichling, Nanotechnology **17**, S148 (2006).
[8] L. Howald, E. Meyer, R. Lüthi, H. Haefke, R. Overney, H. Rudin, and H. J. Güntherodt, Appl. Phys. Lett. **63**, 117 (1993).
[9] L. Howald, H. Rudin, and H. J. Güntherod, Rev. Sci. Instrum. **63**, 3909 (1992).
[10] T. R. Albrecht, P. Grütter, D. Horne, and D. Rugar, J. Appl. Phys. **69**, 668 (1991).
[11] E. R. I. Abraham and E. A. Cornell, Appl. Opt. **37**, 1762 (1998).
[12] S. Gritschneder, Y. Namai, Y. Iwasawa, and M. Reichling, Nanotechnology **16**, S41 (2005).
[13] S. Gritschneder, Y. Iwasawa, and M. Reichling, Nanotechnology **18**, 044025 (2007).
[14] S. Gritschneder and M. Reichling, Nanotechnology **18**, 044024 (2007).
[15] F. J. Giessibl, Appl. Phys. Lett. **76**, 1470 (2000).
[16] M. Abe, Y. Sugimoto, O. Custance, and S. Morita, Appl. Phys. Lett. **87**, 173503 (2005).
[17] T. Fukuma, M. Kimura, K. Kobayashi, K. Matsushige, and H. Yamada, Rev. Sci. Instrum. **76**, 053704 (2005).
[18] T. Fukuma and S. P. Jarvis, Rev. Sci. Instrum. **77**, 043701 (2006).
[19] We use the Dulcinea control unit (Nanotec Electronica, Madrid, Spain) for scanning control and the easy PLL demodulator and sensor controller (Nanosurf, Liestal, Switzerland) for cantilever excitation and signal demodulation.
[20] S. Torbrügge, M. Reichling, A. Ishiyama, S. Morita, and O. Custance, Phys. Rev. Lett. **99**, 056101 (2007).
[21] S. Gritschneder and M. Reichling, J. Phys. Chem. C **112**, 2045 (2008).
[22] I. Horcas, R. Fernandez, J. M. Gomez-Rodriguez, J. Colchero, J. Gomez-Herrero, and A. M. Baro, Rev. Sci. Instrum. **78**, 013705 (2007).
[23] F. Ostendorf, S. Torbrügge, and M. Reichling, Phys. Rev. B **77**, 041405(R) (2008).
[24] T. Eguchi and Y. Hasegawa, Phys. Rev. Lett. **89**, 266105 (2002).
[25] T. Eguchi, Y. Fujikawa, K. Akiyama, T. An, M. Ono, T. Hashimoto, Y. Morikawa, K. Terakura, T. Sakurai, M. G. Lagally, and Y. Hasegawa, Phys. Rev. Lett. **93**, 266102 (2004).
[26] M. Fendrich, T. Kunstmann, D. Paulkowski, and R. Möller, Nanotechnology **18**, 084004 (2007).
[27] M. A. Venegas de la Cerda, J. Abad, A. Madgavkar, D. Martrou, and S. Gauthier, Nanotechnology **19**, 045503 (2008).